Received: 25 March 2019 | Revised: 10 September 2019 | Accepted: 11 September 2019

DOI: 10.1002/glia.23724

GLIA

WILEY

RESEARCH ARTICLE

Heterogeneous fate choice of genetically modulated adult neural stem cells in gray and white matter of the central nervous system

Felix Beyer[1] | Janusz Jadasz[1] | Iria Samper Agrelo[1] | Jessica Schira-Heinen[1] | Janos Groh[2] | Anastasia Manousi[1] | Christine Bütermann[1] | Veronica Estrada[1] | Laura Reiche[1] | Martina Cantone[3] | Julio Vera[3] | Francesca Viganò[4] | Leda Dimou[4] | Hans Werner Müller[1] | Hans-Peter Hartung[1] | Patrick Küry[1]

[1]Department of Neurology, Medical Faculty, Heinrich-Heine-University Düsseldorf, Düsseldorf, Germany

[2]Department of Neurology, Developmental Neurobiology, University Hospital Würzburg, Würzburg, Germany

[3]Laboratory of Systems Tumor Immunology, Department of Dermatology, Universitätsklinikum Erlangen, Erlangen, Germany

[4]Physiological Genomics, Institute of Physiology, Ludwig-Maximilians Universität München, München, Germany

Correspondence
Patrick Küry, Neuroregeneration Laboratory, Department of Neurology, Heinrich-Heine-University, Moorenstraße 5, D-40225 Düsseldorf, Germany.
Email: kuery@uni-duesseldorf.de

Present address
Martina Cantone, Faculty of Mechanical Engineering, Specialty Division for Systems Biotechnology, Technische Universität München, München, Germany

Present address
Leda Dimou, Molecular and Translational Neuroscience, Department of Neurology, Ulm University, Ulm, Germany.

Funding information
Walter and Ilse Rose Foundation; Peek & Cloppenburg Düsseldorf Stiftung; Stifterverband/Novartisstiftung; iBrain; DMSG Ortsvereinigung Düsseldorf und Umgebung e. V.; Christiane and Claudia Hempel Foundation; Deutsche Forschungsgemeinschaft, Grant/Award Numbers: KU1934/5–1, KU1934/2–1

Abstract

Apart from dedicated oligodendroglial progenitor cells, adult neural stem cells (aNSCs) can also give rise to new oligodendrocytes in the adult central nervous system (CNS). This process mainly confers myelinating glial cell replacement in pathological situations and can hence contribute to glial heterogeneity. Our previous studies demonstrated that the p57kip2 gene encodes an intrinsic regulator of glial fate acquisition and we here investigated to what degree its modulation can affect stem cell-dependent oligodendrogenesis in different CNS environments. We therefore transplanted p57kip2 knockdown aNSCs into white and gray matter (WM and GM) regions of the mouse brain, into uninjured spinal cords as well as in the vicinity of spinal cord injuries and evaluated integration and differentiation in vivo. Our experiments revealed that under healthy conditions intrinsic suppression of p57kip2 as well as WM localization promote differentiation toward myelinating oligodendrocytes at the expense of astrocyte generation. Moreover, p57kip2 knockdown conferred a strong benefit on cell survival augmenting net oligodendrocyte generation. In the vicinity of hemisectioned spinal cords, the gene knockdown led to a similar induction of oligodendroglial features; however, newly generated oligodendrocytes appeared to suffer more from the hostile environment. This study contributes to our understanding of mechanisms of adult oligodendrogenesis and glial heterogeneity and further reveals critical factors when considering aNSC mediated cell replacement in injury and disease.

KEYWORDS
glial fate modulation, myelin, neural stem cell, p57kip2, regional heterogeneity, spinal cord injury, transplantation

Felix Beyer and Janusz Jadasz contributed equally to this study.

1 | BACKGROUND

Heterogeneity among oligodendroglial progenitor cells (OPCs) has previously been related to their gray (GM) or white matter (WM) localization in the central nervous system (CNS; (Lentferink, Jongsma, Werkman, & Baron, 2018; Vigano, Möbius, Götz, & Dimou, 2013)). Based on single cell sequencing data, this information has recently been expanded describing regional differences among oligodendroglial cells (Marques et al., 2016) as well toward disease-specific lineages upon demyelination (Falcao et al., 2018; Jäkel et al., 2019). Moreover, new reports point to an additional contribution to myelin repair in the adult CNS from partially lesioned oligodendrocytes (Duncan et al., 2018; Yeung et al., 2019). Besides GM and WM structures, the subventricular zone (SVZ), one of the stem cell niches of the adult brain, represents yet another source for myelinating cells, thus possibly contributing to glial heterogeneity. Adult self-renewing, multipotent neural stem cells (adult neural stem cells [aNSCs]) mainly generate neuroblasts which eventually differentiate into mature neurons of the olfactory bulb or the striatum (Bond, Ming, & Song, 2015; Lim & Alvarez-Buylla, 2016) but were also shown to give rise to new oligodendroglial cells in the corpus callosum following demyelinating events (Brousse, Magalon, Durbec, & Cayre, 2015; Menn et al., 2006; Nait-Oumesmar et al., 1999; Nait-Oumesmar et al., 2007; Picard-Riera et al., 2002; Xing et al., 2014). Signals responsible for neuronal versus glial progeny decisions remain yet to be identified but a number of factors were shown to either inhibit or promote stem cell-dependent oligodendrogenesis (Akkermann, Beyer, & Küry, 2017). In addition, bioinformatics analysis predicts the existence of a number of unexploited signaling pathways acting on niche cells (Azim et al., 2018). Nevertheless, a detailed knowledge about intrinsic regulators and extrinsic influences is needed in order to understand whether and how neural stem cells can be exploited for robust oligodendrocyte replacement, as warranted by WM loss observed in many neuropathologies. It also remains to be shown to what degree activation of endogenous stem/progenitor cells versus supply of exogenous cells (transplantation) is applicable and whether generated cell derivatives correspond to fully myelinating oligodendrocytes or are alike cells only. Likewise, little is known about the influence of regional differences (GM and WM) as well as of an injury environment on transplanted aNSCs. As previous stem cell transplantation studies revealed poor fate directing properties when NSCs were, for example, instructed to differentiate into neurons prior to transplantation (Koutsoudaki et al., 2016) or when cells overexpressed IGF-1 (Miltiadous et al., 2013), this supports a potential dominant effect of the host tissue.

The p57kip2/cdkn1c gene encodes one of the intrinsic regulators involved in oligodendroglial cell fate acquisition. We previously demonstrated that short-hairpin RNA (shRNA) mediated suppression of this gene in rat aNSCs, derived from the subgranular zone and SVZ stem cell niches, induces oligodendroglial features at the expense of astrocyte generation, notably despite the presence of strong astrogenic cues (Jadasz et al., 2012). In addition, there is evidence for a differential expression of p57kip2 along SVZ subregions correlating with variations in the extent of oligodendrocyte progeny generation (Akkermann et al., 2017). In the current study, we investigated whether this intrinsic fate modulation leads to the same degree of oligodendrocyte formation following aNSC transplantation into different healthy brain and spinal cord regions and whether it can also dominate over factors emanating from a hostile, pathophysiological environment. To this end, genetically modulated aNSCs were transplanted into cortex (GM) and corpus callosum (WM), GM and WM of the spinal cord as well as in the vicinity of acutely lesioned spinal cords in order to investigate differential instructive signals influencing survival, tissue integration, and oligodendroglial differentiation. While we show that also in mouse, SVZ-derived aNSCs p57kip2 knockdown generally induces an oligodendroglial fate we nevertheless detected remarkable differences between WM and GM grafted cells as well as a differential impact from the injury environment on grafted cell survival. Taken together, our results uncover heterogeneous oligodendroglial fate determining and maturation effects mediated by extrinsic and intrinsic regulators.

2 | MATERIAL AND METHODS

2.1 | Animals

Female mice (C57Bl/6) and rats (RjHan:W) were used as host animals in order to avoid possible gender dependent heterogeneity. All rodents were housed in a pathogen-free facility with 12 hr light/dark cycle and supplied with food/water ad libitum. Transplantation experiments into wildtype mice and rats were all approved by the LANUV (Landesamt für Natur, Umwelt und Verbraucherschutz Nordrhein-Westfalen; Az.: 84-02.04.2015.A239; Az.: 84-02.04.2015.A525) and carried out in accordance with ethical care. For the preparation of adult mouse NSCs from wildtype C57Bl/6 or transgenic (NesCreERT2::tdTomato) mice 3 month old female animals were used. Please note that NesCreERT2::tdTomato mice were received by introducing an inducible tdTomato cassette (Gt(ROSA)26Sor locus; for further detail, please see Jackson Laboratory stock No. 007914) into NesCreERT2 mice (Imayoshi, Ohtsuka, Metzger, Chambon, & Kageyama, 2006). Rat aNSCs were prepared from 8 to 10 week old female Wistar rats.

2.2 | Adult mouse and rat neural stem cell culture and transfection

Preparation of aNSCs was conducted using adult mouse and rat SVZs as previously described (Jadasz et al., 2012; Jadasz et al., 2018). Briefly, isoflurane anesthetized animals were killed by decapitation and after removal of the brains SVZ of both hemispheres were prepared, mechanically digested and transferred to 4°C phosphate buffered saline (PBS; D8537; Sigma-Aldrich, Taufkirchen, Germany). After washing in PBS, cells were enzymatically digested in PDD solution containing papain (0.01%, Worthington Biochemicals, Lakewood, CA), Dispase II (0.1%, Boehringer, Ingelheim, Germany), DNase I (0.01%, Worthington Biochemicals), and 12.4 mM MgSO4, dissolved in HBSS (PAA Laboratories) for 30 min at 37°C with trituration steps every 10 minutes. After additional washing steps in neurobasal (NB) medium

(Gibco BRL, Karlsruhe, Germany) supplemented with B27 (Gibco), 2 mM L-glutamine (Gibco), 100 U/mL penicillin/0.1 mg/L streptomycin (Gibco) and centrifugation at 140 rcf for 5 min, cells were resuspended in NB medium supplemented with 2 mg/mL heparin (Sigma-Aldrich), 20 ng/mL FGF-2 (R&D Systems, Wiesbaden-Nordenstadt, Germany), and 20 ng/mL EGF (R&D Systems) from here on referred to as NBall medium. Cells were seeded at 1×10^6 cells in one T75 culture flask in 10 mL NBall medium and cultured for 7 days at 37°C in a humidified incubator with 5% CO_2. The medium was exchanged twice a week and on Day 7 cells were passaged using accutase (PAA Laboratories) for separation (10 min at 37°C). Mouse and rat aNSCs were dispersed using an accutase step and subjected to nucleofection using a Lonza nucleofection device and the adult mouse NSC nucleofector kit (Lonza, Basel, Switzerland) as described before (Jadasz et al., 2018). Briefly, 4×10^6 cells were transfected using the program A-033 (high efficiency) resuspended in 100 μL nucleofection solution and 10 μg plasmid DNA. Nucleofections were performed using constructs pSUPER ("ctrl"; empty vector control) and pSUPER-p57kip2 ("p57-KD"; suppression of p57kip2) and for visualization of transfected cells a citrine expression vector was cotransfected at a ratio of 5:1 all as published previously (Heinen et al., 2008; Jadasz et al., 2012; Kremer et al., 2009). Transfected cells were plated on poly-L-ornithine/laminin (100 and 5 μg/mL; Sigma-Aldrich) coated and acid pretreated 13 mm glass cover slips (8×10^4 cells/coverslip) for 24 hr in NBall medium before changing to astrocyte fate stimulating medium (Minimum Essential Medium Alpha (α-MEM) supplemented with 10% fetal calf serum (FCS)). For in vitro quantitative real-time reverse transcription PCR (qRT-PCR) analysis, transfected cells were first cultured in 10 mL NBall medium for 24 hr in T75 flasks. Prior to fluorescent activated cell sorting (Jadasz et al., 2012), cells were gently washed from the flasks, treated for 5 min with accutase, washed with PBS containing 2 mM ethylenediaminetetraacetic acid, and subsequently sorted by means of citrine expression. Sorted cells were plated on 13 mm glass cover slips and cultured in α-MEM + 10% FCS medium. For in vivo transplantation experiments, cells (derived from transgenic tdTomato-positive mice or from wildtype rats) were transfected as described above 1 hour prior to grafting.

2.3 | Immunocytochemistry

α-MEM + 10% FCS cultured mouse aNSCs were fixed after 4 or 7 days using 4% paraformaldehyde (PFA) and stained for the detection of marker proteins as previously described (Jadasz et al., 2018) using the following antibodies: rabbit anti-neural/glial antigen 2 (NG2; 1:100, AB5320, Millipore, RRID: AB_11213678), rabbit anti-glutathione-S-transferase-π (GSTπ; 1:500, ADI-MSA-101, ENZO, RRID: AB_10615079) and rabbit anti-glial fibrillary acidic protein (GFAP; 1:4000, Z0334, DAKO, RRID: AB_10013382). Primary antibodies were incubated at 4°C overnight, followed by three washing steps (1x PBS) and incubation with the secondary antibody (goat anti-rabbit Alexa 594; 1:500; A-11037, Thermo Fisher Scientific, RRID: AB_2534095) in PBS (supplemented with 4′,6-diamidin-2-phenylindol [DAPI]) at room temperature (RT) for 30 min. Images were taken using a Zeiss Axioplan2 microscope and analyzed using the ImageJ BioVoxxel software.

2.4 | Gene expression analysis

Transfected and sorted mouse aNSCs were lysed after 7 days using 350 μL RLT lysis buffer (Qiagen) supplemented with β-mercaptoethanol (1:100, Sigma). Total RNA purification, cDNA synthesis, and qRT-PCR were performed as previously described (Jadasz et al., 2012). For sequence detection, the following forward (fwd) and reverse (rev) primers were used, with TBP and ODC serving as reference genes:

TBP_fwd: AGAATAAGAGAGCCACGGACAACT, TBP_rev: TGGCTCCTGTGCACACCAT; ODC_fwd: GGTTCCAGAGGCCAAACATC, ODC_rev: GTTGCCACATTGACCGTGAC; p57kip2_fwd: CCGACTGAGAGCAAGCGAAC, p57kip2_rev: ATTGGTGATGGACGGCTCCT; NG2_fwd: ACGATCCACCTCGCATCATC, NG2_rev: GTTCCACAGGGACACCAGAG; GSTπ_fwd: CATGCCACCATACACCATTGTC, GSTπ_rev: CATTCGCATGGCCTCCA; nestin_fwd: AGCCATTGTGGTCTACGGAAGT, nestin _rev: TCCACACACCCCAGTGGTT; Hes5_fwd: TGCAGGAGGCGGTACAGTTG, Hes5_rev: GCTGGAAGTGGTAAGCAGCTT; GFAP_fwd: CCAGCTTCGAGCCAAGAA, GFAP_rev: GAAGCTCCGCCTGGTAGACA; AQP4_fwd: TCCTGATGTGGAGCTCAAACG, AQP4_rev: GCTGCGCGGCTT TGC; Sox2_fwd: CCAGCGCATGGACAGCTA, Sox2_rev: GCTGCTCCTGCATCATGCT.

2.5 | Stereotactic transplantation into GM and WM of the mouse brain

Then, 1 hr prior to transplantation, mouse aNSCs were transfected as described above and kept at RT in PBS. For transplantation into the mouse brain, cells were centrifuged for 5 min at 140 rcf and resuspended in PBS to a density of 1×10^5 cells/μL. Recipient C57Bl/6J mice were deeply anesthetized using isoflurane inhalation. Approximately 0.75 μL of the cell suspension was injected in either the WM or GM of the somatosensory cortex of (13–14 week old) mice according to Vigano et al. (2013). Transplantations were performed with a Hamilton syringe (10 μL Neuros Model 1701 RN, ga 33, *L* 0–20 mm) into the WM at 0.7 mm (anterior–posterior), ±1 mm (medial–lateral), 2.1–1.8 mm (dorsal–ventral) relative to the bregma and into the GM at 0.7 mm (anterioposterior), ±1 mm (medial–lateral), 1.5–1.3 mm (dorsal–ventral) relative to the bregma using a motorized robot stereotaxic instrument and StereoDrive software (Neurostar). Postoperative care comprised an analgesic treatment (RIMADYL, Pfizer; 5 mg/kg) for 3 days starting on the day of operation. For tissue removal, mice were deeply anesthetized with isoflurane and transcardially perfused with 20 mL ice-cold PBS followed by 20 mL 4% PFA. Mouse brains were harvested and postfixed overnight in 4% PFA at 4°C, followed by 24–48 hr cryoprotection in 30% sucrose (in PBS) at 4°C. Brains were embedded in Tissue-Tek OCT (Sakura Finetek Europe, Netherlands), frozen, and stored at −80°C until preparation of 10 μm sections using a cryostat (Leica CM3050S). Sections were stored at −80°C.

2.6 | Stereotactic transplantation into the intact and hemisected rat spinal cord

Adult female rats were operated as previously described (Schira et al., 2012) with slight modifications. Briefly, after dorsal hemisection at thoracic level eight (Th8) using a Scouten wire knife (Bilaney), the dura was sutured and then rat aNSC transplantation was performed using a glass capillary, attached to a Small Animal Stereotaxic Instrument (David Kopf Instruments), at 2 mm rostral and 2 mm caudal to the lesion, 0.1 mm lateral to the midline and 1.1 mm (for GM) or 0.7 mm (for WM) dorsal–ventral from the dural surface. For the transplantation of aNSCs into the intact spinal cord, no hemisection was performed but cells were implanted at the same coordinates as previously mentioned. At each transplantation site 2 μL containing 1×10^5 either control transfected (ctrl; empty vector) or p57kip2-suppressed (p57-KD) cells in PBS were injected slowly within 4 min. Cells were transfected 60 min prior to grafting and for cell detection a citrine expression vector was cotransfected as indicated above. Please note that for both conditions, control and p57-KD, transfection efficiency was comparably high (Supplementary Figure 2). Postoperative care included prophylactic oral antibiotic treatment (Baytril, Bayer Health Care; 0.4 mL/kg) and manual bladder expression for 1 week. Further to this, rats received an analgesic treatment (RIMADYL, Pfizer; 5 mg/kg) for 3 days starting on the day of operation. Seven days postoperation, animals were transcardially perfused. Rats were deeply anesthetized using a mixed solution containing Ketamine (100 mg/kg body weight) and xylazine (10 mg/kg body weight) and transcardially perfused with 200 mL 4°C PBS followed by 400 mL 4% PFA. Spinal cords were harvested and postfixed overnight in 4% PFA at 4°C, followed by 24–48 hr cryoprotection in 30% sucrose (in PBS) at 4°C. Spinal cords were then embedded in Tissue-Tek OCT (Sakura Finetek Europe), frozen, and stored at −30°C until preparation of 10 μm sections using a cryostat (Leica, CM3050S). Sections were stored at −30°C.

2.7 | Immunohistochemistry

Brain and spinal cord sections were thawed and left to dry for at least 15 min at RT. Before blocking, sections were rehydrated for 5 min in distilled water, transferred to −20°C acetone (5 min), and washed in 1x TBS (pH 7.6) and 1x TBS-T (TBS containing 0.02% Triton) for 5 min each. Blocking was performed with 5–10% biotin-free bovine serum albumin (BSA; in TBS-T) for 30 min at RT, followed by application of the following antibodies (in 5–10% BSA in TBS) and incubation overnight: rabbit anti-NG2 (1:100; MAB5320; Millipore, RRID: AB_11213678; RT), rabbit anti-sex determining region Y-Box 10 (Sox10; 1:100, S1058C002, DCS Immunoline, RRID: AB_2313583; RT), rabbit anti-GFAP (1:10,000; Z0334, DAKO, RRID: AB_10013382; 4°C), goat anti-doublecortin (Dcx; 1:100, sc-8066, Santa Cruz, RRID: AB_2088494; 4°C), rabbit anti-GSTπ (1:4,000; ADI-MSA-101, ENZO, RRID: AB_10615079; 4°C), mouse anti-2′,3′-cyclic-nucleotide 3′-phosphodiesterase (CNPase; 1:5,000, 836,402, Biolegend, RRID: AB_2565362; 4°C), rat anti-myelin basic protein (MBP; 1:500, MCA409S, BioRad, RRID: AB_325004; 4°C), rabbit anti-NeuN (1:500; ab177487, Abcam, RRID: AB_2532109; 4°C), mouse anti-myelin oligodendrocytes glycoprotein (MOG; 1:500, MAB5680, Millipore, RRID: AB_1587278; 4°C), and chicken anti-green fluorescent protein/citrine (1:500–2,000; GFP-1020, Aves, RRID: AB_10000240; 4°C or RT). Sections were washed two times for 7.5 min in TBS and incubated with the species-appropriate fluorochrome-conjugated secondary antibody (1:500 in PBS) for 30 min at RT: donkey anti-chicken Alexa 488 (703-545-155, Jackson Immuno Research Labs, RRID: AB_2340375), donkey anti-goat Alexa 647 (A-21447, Thermo Fisher Scientific, RRID: AB_2535864), goat anti-chicken Alexa 488 (A-11039, Thermo Fisher Scientific, RRID: AB_2534096), goat anti-rabbit Alexa 405 (A-31556, Thermo Fisher Scientific, RRID: AB_221605), goat anti-mouse Alexa 647 (A-32728, Thermo Fisher Scientific, RRID: AB_2633277), goat anti-rat Alexa 647 (A-21247, Thermo Fisher Scientific, RRID: AB_141778), goat anti-rabbit Alexa 594 (A-11037, Thermo Fisher Scientific, RRID: AB_2534095), and DAPI or RedDot 2 (Biotium, Cat.#: 40061). Images were taken using a Zeiss CLSM microscope 510 (CLSM 510, Zeiss, Jena, Germany) and analyzed using the ImageJ BioVoxxel software.

2.8 | Histological cell quantification

Immunohistochemical staining was done on brain sections of the corresponding centers of transplantation (on average, 25 sections per marker per time point were analyzed). Fluorescently marked cells were counted on each picture/section leading to an average value for each animal. Observed cell numbers are represented by the area of an individual circle (Figure 3). For quantification of cell numbers in spinal cord, transplantation experiments corresponding centers of transplantation were used and 14–24 sections encompassing the transplantation zone per animal were analyzed. After calculating the mean number of citrine-positive cells per section, this number was then multiplied with the total number of sections containing citrine-positive cells (between 40 and 65 sections per animal) to indicate total numbers of surviving cells in the spinal cord.

2.9 | Immunoelectron microscopy

For immunoelectron microscopy, mice were perfused with 4% PFA in cacodylate buffer, brains were dissected and postfixed overnight. Brains were embedded in 6% agarose in cacodylate buffer, and 50-μm-thick coronal sections were cut in PBS using a microtome (Microm HM 650 V, Thermo Fisher Scientific). Free-floating sections were blocked with 1% BSA in PBS and incubated with 0.1 M $NaIO_3$ in PBS and subsequently in 5% dimethyl sulfoxide in PBS. Sections were incubated with rabbit anti-GFP antibody (1:100; AB3080, Millipore, RRID:AB_91337) in 1% BSA in PBS overnight at 4°C and immune reactions were subsequently visualized using a biotinylated secondary antibody (biotinylated goat anti-rabbit IgG; 1:50; BA-1000, Vector, RRID: AB_2313606) and streptavidin-biotin-peroxidase (PK-6100, Vector Laboratories, RRID:AB_2336819) complex using diaminobenzidine–HCl (SK-4105, Vector Laboratories, RRID:AB_2336520) and H_2O_2. After diaminobenzidine staining, appropriate regions of the corpus callosum were cut, the sections were osmicated and processed for light and electron microscopy by dehydration and embedding in Spurr's medium.

Ultrathin sections (70 nm) were mounted to copper grids, counterstained with lead citrate, and investigated using a ProScan Slow Scan CCD camera mounted to a Leo 906 E electron microscope (Zeiss) and corresponding software iTEM (Soft Imaging System).

2.10 | Statistical analysis

Statistical analyses and graphs were done using Excel and Graph-Pad Prism 5.0 software. To determine statistical significance in graphs with more than two conditions, ordinary (not repeated measures) two-way analysis of variance with Bonferroni posttest was applied. For datasets with two conditions, Student's two-sided, unpaired *t* test was applied. Statistical significance thresholds were set as follows: $*p < .05$; $**p < .01$; $***p < .001$. All data are shown as mean values ± *SEM* and "*n*" represents the number of independent experiments performed.

3 | RESULTS

3.1 | p57kip2 gene suppression leads to oligodendroglial fate acquisition in cultured aNSCs

The p57kip2/cdkn1c gene has previously been shown to encode a negative regulator of Schwann cell and oligodendroglial precursor cell differentiation (Heinen et al., 2008; Kremer et al., 2009). Moreover, we demonstrated that enforced downregulation of p57kip2 expression leads to accumulation of oligodendroglial features and markers in rat hippocampus-derived aNSCs (Jadasz et al., 2012). Please note that in this previous publication, we demonstrated that p57kip2 suppression induces a moderate survival benefit in aNSCs and that it also slightly promoted their proliferation. In order to prepare in vivo stem cell maturation studies, we conducted a series of experiments using cultured adult mouse SVZ-derived NSCs. To assess whether p57kip2 gene suppression also instructs an oligodendroglial fate in mouse aNSCs, we transfected them with a p57kip2 specific shRNA generating vector (p57-KD; Heinen et al., 2008; Jadasz et al., 2012; Kremer et al., 2009). Control cells were transfected with an empty expression vector and for identification of transfected cells, a citrine-encoding construct was cotransfected. Transfected cells were fluorescence-activated cell sorted by means of their citrine expression (Jadasz et al., 2012) 1 day following transfection and subsequently cultured in an astroglial fate promoting medium as described previously (Jadasz et al., 2012; Jadasz et al., 2018). Seven days following transfection, transcript levels were measured and suppression of p57kip2 was confirmed (Figure 1a). This was accompanied by an increased gene expression of NG2 (oligodendroglial precursor marker; Figure 1b) and of the mature oligodendrocyte marker GSTπ (Figure 1c). At the same time, the expression of the negative regulator of oligodendroglial differentiation Hes5, of astroglial GFAP and aquaporin-4 (AQP4) and of stem cell markers nestin and Sox2 was decreased (Figure 1d-h). For validation of RNA expression, immunocytochemical staining using antibodies directed against NG2 (4d), GSTπ

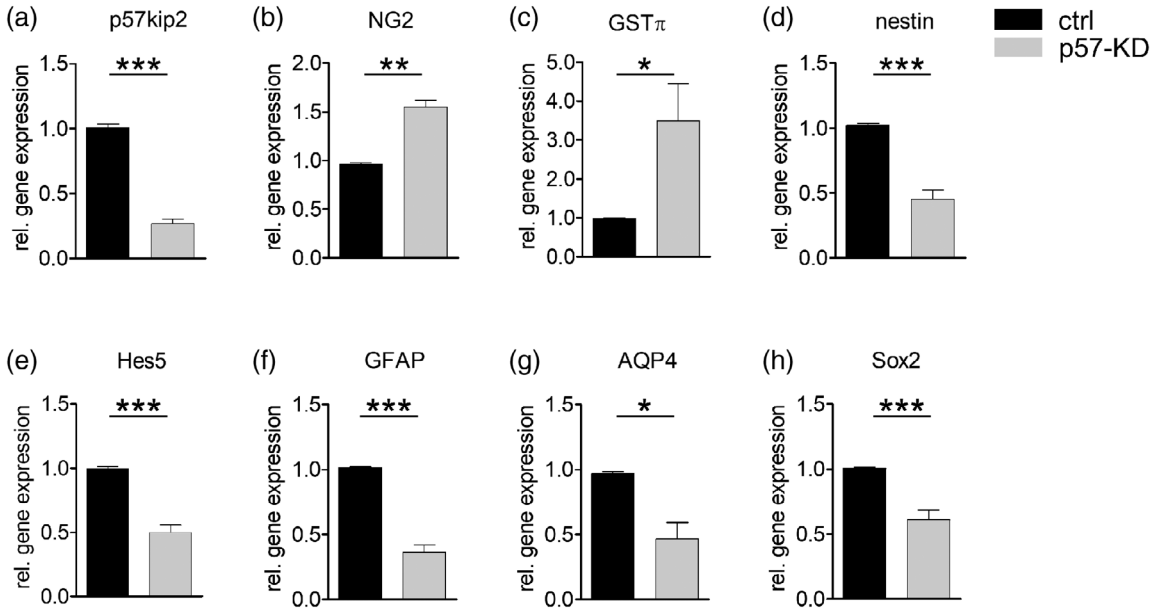

FIGURE 1 Increased oligodendroglial gene expression in adult NSCs following suppression of p57kip2. qRT-PCR of FACS-sorted aNSCs 7 days following shRNA-mediated suppression of p57kip2 (p57-KD; gray bars) revealed p57kip2 transcript level reduction (a) compared to control transfected cells (ctrl; black bars). This led to an increased expression of early (NG2; b) as well as of mature oligodendroglial marker genes (GSTπ; c). The increase in oligodendroglial gene expression was accompanied by a decreased expression of stem cell genes nestin (d) and Sox2 (h), of the oligodendroglial differentiation inhibitor Hes5 (e), and of the astrocytic marker genes GFAP (f) and AQP4 (g). Data are shown as mean values, error bars represent *SEM*. Number of independent experiments: $n = 3$ for (b,g), $n = 4$ for (d), $n = 5$ for (c,h,f), and $n = 6$ for (a,e). Statistical significance was calculated using Student's two-sided, unpaired *t* test: $*p < .05$; $**p < .01$; $***p < .001$. aNSCs, adult neural stem cells; FACS, fluorescent activated cell sorting; GFAP, glial fibrillary acidic protein; GSTπ, glutathione-S-transferase-π; qRT-PCR, quantitative real-time reverse transcription PCR; shRNA, short-hairpin RNA

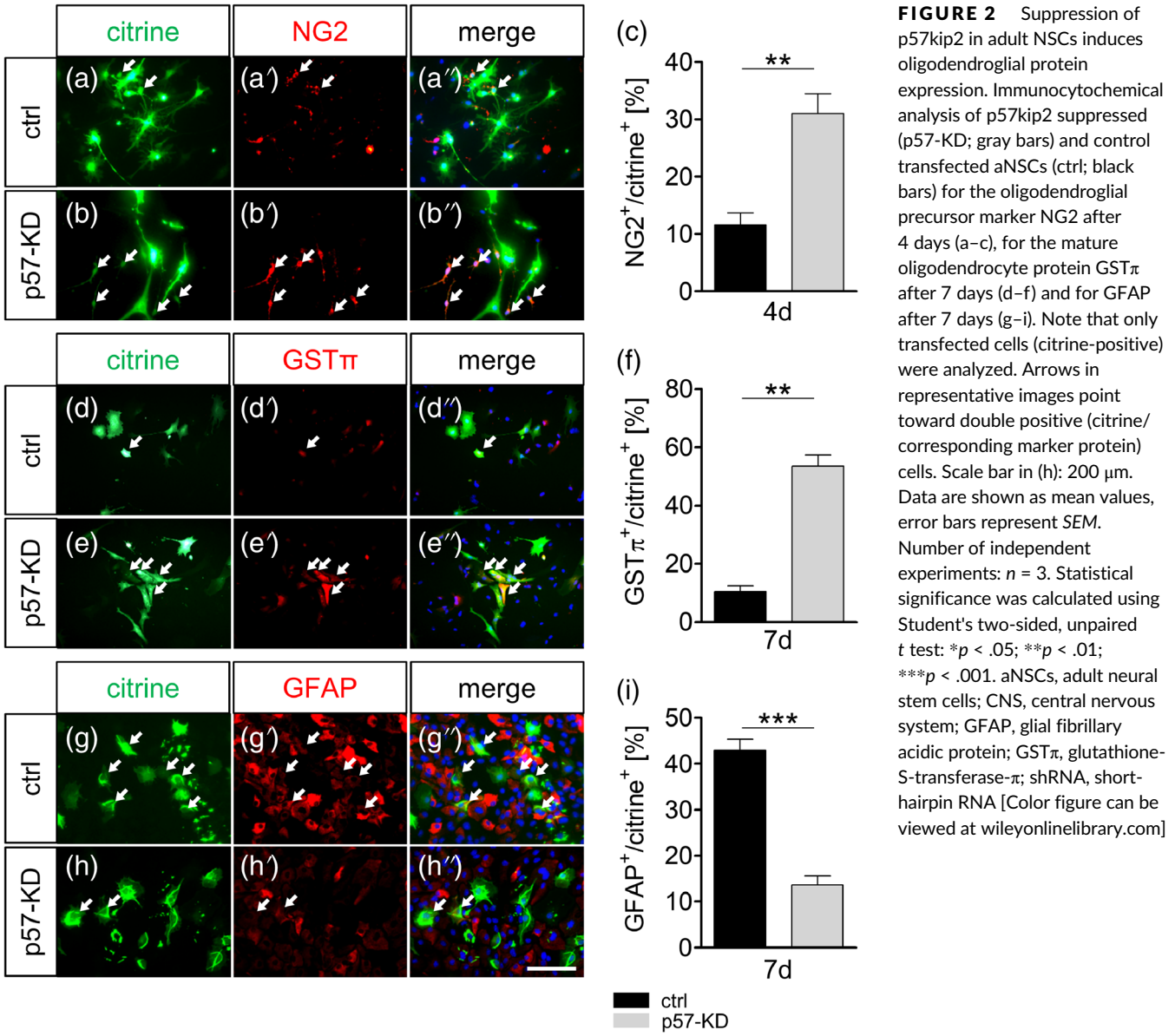

FIGURE 2 Suppression of p57kip2 in adult NSCs induces oligodendroglial protein expression. Immunocytochemical analysis of p57kip2 suppressed (p57-KD; gray bars) and control transfected aNSCs (ctrl; black bars) for the oligodendroglial precursor marker NG2 after 4 days (a–c), for the mature oligodendrocyte protein GSTπ after 7 days (d–f) and for GFAP after 7 days (g–i). Note that only transfected cells (citrine-positive) were analyzed. Arrows in representative images point toward double positive (citrine/corresponding marker protein) cells. Scale bar in (h): 200 μm. Data are shown as mean values, error bars represent *SEM*. Number of independent experiments: $n = 3$. Statistical significance was calculated using Student's two-sided, unpaired *t* test: $^{*}p < .05$; $^{**}p < .01$; $^{***}p < .001$. aNSCs, adult neural stem cells; CNS, central nervous system; GFAP, glial fibrillary acidic protein; GSTπ, glutathione-S-transferase-π; shRNA, short-hairpin RNA [Color figure can be viewed at wileyonlinelibrary.com]

(7d), and GFAP (7d) were performed. Only transfected cells (marked by citrine expression) were scored and quantification confirmed increased oligodendroglial identities at the expense of GFAP expression in p57kip2 suppressed aNSCs (Figure 2).

Having established that transfection of the p57kip2 suppression vector confers an oligodendroglial fate on mouse SVZ-derived aNSCs as compared to control transfected cells (ctrl), we next investigated how to accomplish in vivo transplantation experiments with the lowest degree of technical variance among different host animals and surgeries. We therefore examined whether SVZ-derived aNSCs from transgenic tdTomato expressing mice (driven by nestin promoter (Imayoshi et al., 2006)) showed similar (p57kip2 dependent) properties in terms of oligodendroglial fate choice as nontransgenic transfected cells. For this purpose, we used a transgenic reporter mouse line in which the tdTomato expression was observed in approximately 50% of the cultured aNSCs (data not shown) as additional source for the preparation of SVZ aNSCs. Transfection of the p57kip2 suppression vector/citrine vector combination reproducibly resulted in a third of cells being citrine-positive (of which 50% were also tdTomato-positive), hence with knocked down p57kip2 levels, whereas another third of cells was tdTomato-positive only. In our in vivo approaches, we then strictly compared green to red-only cells in order to have a site-by-site comparison of p57kip2 suppressed compared to control aNSCs. Note that cultured nontransfected/wildtype aNSCs, control-transfected/wildtype aNSCs and nontransfected/tdTom-positive (transgenic) aNSCs showed the same astroglial and oligodendroglial protein marker expression dynamics (Supplementary Figure 1). Immunocytochemistry revealed that the degree of nestin positivity was the same (100%) in both, wildtype and tdTom-positive, stem cell populations. In addition, GFAP, GSTπ, and Hes5 gene expression analysis revealed the same p57-KD-dependent expression dynamics as shown for transfected wildtype aNSCs (Supplementary Figure 3). We also transplanted this cell population onto myelinating cocultures (Göttle et al., 2015; Göttle et al., 2018) in order to provide an as much as possible physiological ex vivo

environment. These experiments revealed that suppression of p57kip2-induced Sox10 expression, a marker expressed in the whole oligodendrocytic lineage, in transgenic (tdTomato-positive) aNSCs from 14.63% ± 0.84% to 30.37% ± 2.17% which was to a similar degree as when control transfected wildtype aNSCs were compared to p57-KD transfected wildtype aNSCs (data not shown). This provided strong evidence that a direct assessment of citrine-positive (p57-KD) versus tdTomato-only-positive (ctrl) cells perfectly reflects the differences as previously seen when p57-KD transfected cells were compared to control transfected cells. This constitutes an important aspect as we aimed at comparing cell fates upon modulation of p57kip2 expression in each individual host animal in situ, hence with a minimum of variation arising from the use of different mice or injection sites.

3.2 | p57kip2 suppressed aNSCs show survival advantage in both, GM and WM

As a next step, transgenic (tdTomato-positive) aNSCs transfected with the p57-KD/citrine vector combination were transplanted into 13–14 week old mouse brains. Coordinates were chosen according to a previous study challenging the fate of grafted OPCs (Vigano et al., 2013) and modulated aNSCs were either implanted into WM or GM regions (corpus callosum and neocortex, respectively). Note that every graft was composed of tdTomato-only-positive control cells and of cells with downregulated p57kip2 expression (citrine-positive). Counting the number of fluorescent cells at 4, 14, and 42 days post-transplantation (dpt) revealed differences in cell survival rates depending on the genetic modulation and site of transplantation (as presented as pie charts in Figure 3). Overall, p57kip2 suppressed aNSCs showed greater survival rates as compared to control cells in both GM and WM, and at all time points examined. Such an increased survival upon p57kip2 knockdown, despite the fact that these cells underwent nucleofection, suggests that gene suppression or the subsequently induced oligodendroglial fate acquisition confer a survival benefit. Over time, a modest decline in surviving cell numbers was observed which was less prominent in WM as compared to GM (compare Figure 3c to b). Furthermore, the survival benefit of p57-KD cells appeared to increase over time. Importantly, because cell counts were not generated by means of a longitudinal analysis but derived by examining tissues from different cohorts of grafted mice, a direct comparison in numbers is only possible between GM and WM at a single time point but not within a given tissue between different time points. Nevertheless, using the here presented grafting procedure, we were able to reproducibly generate mice with implanted, genetically modified cells over a period of up to 6 weeks, thus allowing detailed analysis of maturation in vivo and tissue integration.

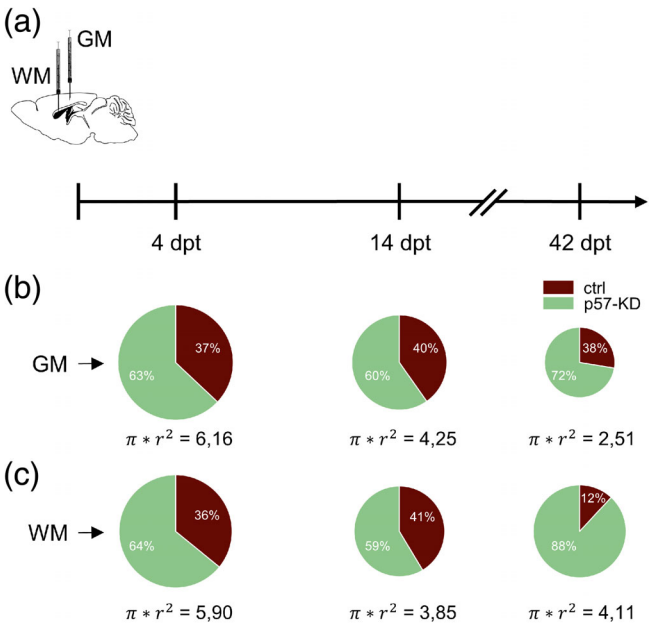

FIGURE 3 WM tissue and suppression of p57kip2 support survival of transplanted adult NSCs. (a) aNSC transplantation set up into GM or WM (GM, WM) and time points (ctrl: tdTomato-only-positive nontransfected cells; p57-KD: citrine-positive p57kip2 suppressed cells). Grafting into GM (b) and WM (c) of young adult mouse brains. Brains were analyzed 4, 14, or 42 days posttransplantation (dpt). (b,c) Area ($A = \pi r^2$) of pies represent the average cell count per field of view following all immunohistochemical analyses for each time point and tissue (GM vs. WM). Average survival rates of p57-KD cells (green) and ctrl cells (red) are given in percent within each pie. aNSCs, adult neural stem cells; GM, gray matter; WM, white matter [Color figure can be viewed at wileyonlinelibrary.com]

3.3 | WM signals and suppression of p57kip2 promote oligodendroglial fate choice

In order to determine the impact of a modulated p57kip2 expression in addition to GM versus WM environmental cues on fate acquisition of adult NSCs, brain sections (4, 14, and 42 dpt) were subjected to immunofluorescent staining (Figures 4 and 5). Quantitative analysis revealed that at 4 dpt Sox10 protein could only be detected in WM implanted cells or in GM implanted cells when they were p57kip2 suppressed (Figure 4b–d‴,l). In the WM, the number of Sox10-positive cells was further increased by p57kip2 knockdown. A similar induction of NG2 positivity was observed in response to p57kip2 suppression at 4 dpt in both tissues (Figure 4e–g‴,m). Note that at this stage, both tissues featured comparable numbers of implanted cells as represented by the pie charts in Figure 3. Concomitantly, the expression of GFAP was significantly decreased due to the p57kip2 knockdown at 4 dpt, whereas levels were generally lower in the WM (Figure 4h–i‴,n). To test for a possible early neuronal fate, brain sections were stained using an antibody directed against the neuroblast marker Dcx. Neither suppression of p57kip2 nor tissue specific effects led to significant differences in the ratio of transplanted aNSC-derived neuroblasts (Figure 4j–k‴,o).

We next examined expression of the mature oligodendrocyte marker GSTπ among transplanted aNSCs at 14 dpt (Figure 5b–e). Generally, GSTπ was found to be expressed in more cells transplanted into the WM, we nevertheless observed a robust and significant induction in response to the p57kip2 knockdown. On the other hand,

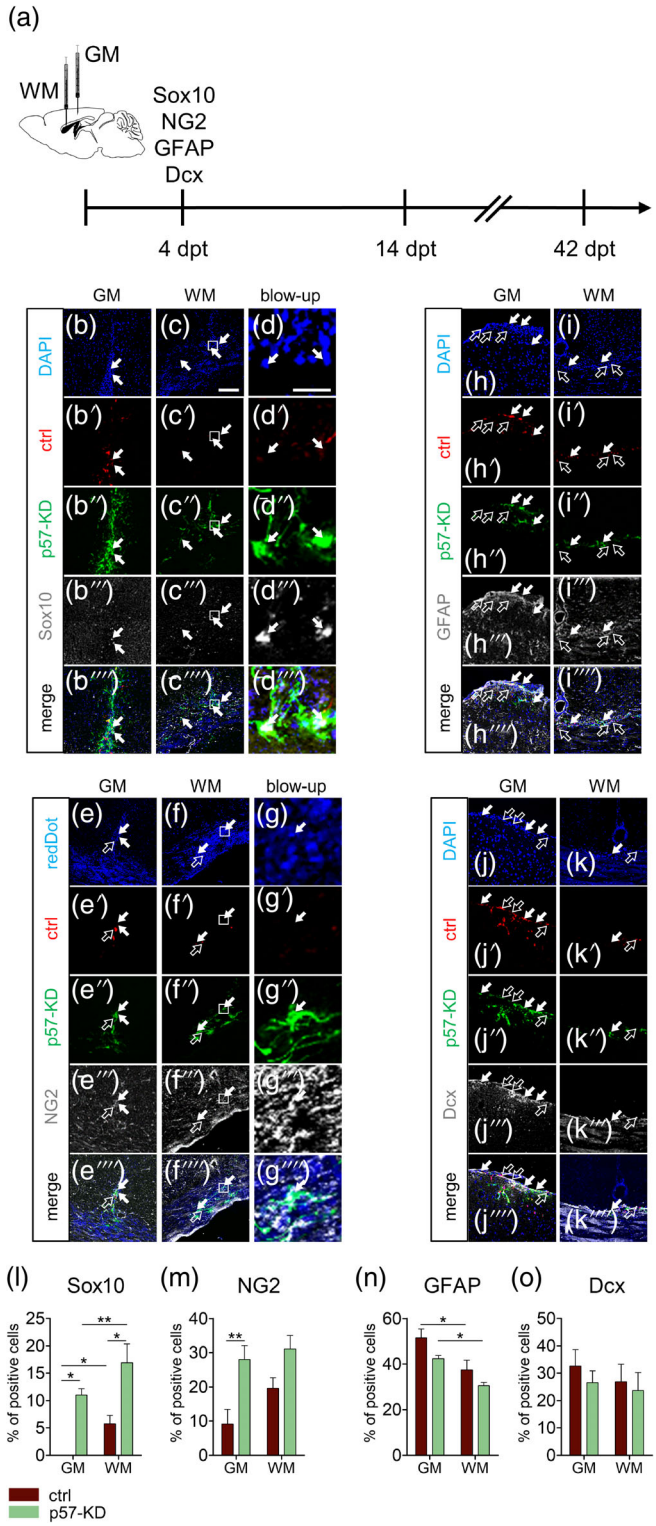

FIGURE 4 Conferring an oligodendroglial fate to adult NSCs in vivo following suppression of p57kip2 and transplantation into WM tissue. (a) aNSC transplantation set up into GM or WM, time point, and examined marker proteins (ctrl: tdTomato-only-positive nontransfected cells; p57-KD: citrine-positive p57kip2 suppressed cells). (b–o) Immunohistochemical analysis for Sox10, NG2, GFAP, and Dcx was performed 4 days posttransplantation to reveal early fate choices of transplanted aNSCs. While oligodendroglial and astroglial marker protein expression correlate inversely, expression of Dcx showed neither tissue nor p57kip2-dependent changes. Inserts in (c–c‴′) and (f–f‴′) correspond to blow-ups in (d–d‴′) and (g–g‴′), respectively. White arrows point toward citrine- and Sox10-/NG2-/GFAP-/Dcx- double-positive cells, respectively, while open arrows point toward tdTomato- and NG2-/GFAP-/Dcx- double-positive cells, respectively. Scale bar in (c) for all nonblow up pictures: 100 μm. Scale bar in (d) for all blow-ups: 20 μm. Data are shown as mean values, error bars represent *SEM*. Number of independent experiments: $n = 5$ animals per graft site. Statistical significance was calculated using two-way ANOVA with Bonferroni posttest: $*p < .05$; $**p < .01$. ANOVA, analysis of variance; aNSCs, adult neural stem cells; GFAP, glial fibrillary acidic protein; GM, gray matter; WM, white matter [Color figure can be viewed at wileyonlinelibrary.com]

at this time point, reduction in GFAP-positivity was more pronounced among WM implanted cells (Figure 5f). Finally, in order to test for functional integration including stem cell-derived myelin protein expression and the establishment of myelin sheaths, transplanted cells were analyzed at 42 dpt, mainly focusing on WM. We examined to what degree p57kip2 knockdown also confers a benefit in myelination when cells were exposed to axons in vivo. Moreover, we also wanted to address the question whether aNSCs after being cultured for several passages in vitro still have the potential to fully differentiate into myelinating oligodendrocytes following transplantation. Brain sections were subjected to immunofluorescent staining using antibodies against myelin proteins CNPase, MBP, and MOG. In WM, a strong increase in the degree of myelin protein expressing cells was detected in response to the long-term p57kip2 knockdown (Figure 5g–j). Note that a comparison between GM and WM, which was conducted using MOG stained cells, revealed that p57kip2 suppression boosts myelin expression in both tissues (Figure 5j). Furthermore, overall induction levels were higher in WM and together with the fact that at this time point significantly more p57kip2-suppressed cells survived in WM as compared to GM (see Figure 3), the overall yield in mature myelinating oligodendrocytes was severely elevated in this condition. These cells also displayed multiple myelin positive cell extensions morphologically resembling mature oligodendrocytes (Figure 5g–g‴; i–iv). An initial qualitative electron microscopic analysis further confirmed that processes of transplanted p57kip2-suppressed cells, identified by means of electron dense phenazine precipitates derived from anti-citrine immunohistochemical detection, were indeed found in direct proximity to myelin sheaths around corpus callosum axons. These myelinating extensions are therefore likely to derive from transplanted aNSC-derived oligodendrocytes (Figure 5k–m). The degree of actively myelinating cells out of the pool of p57kip2 suppressed cells, over time as well as in relation to their integration sites, should be determined in upcoming studies.

3.4 | Stem cell-derived oligodendrogenesis in the spinal cord

In order to test whether the observed pro-oligodendroglial behavior of modulated stem cells is maintained under hostile conditions, aNSCs were transplanted into the lesioned spinal cord. For practical reasons, rat spinal cord hemisection characterized by a profound local lesion

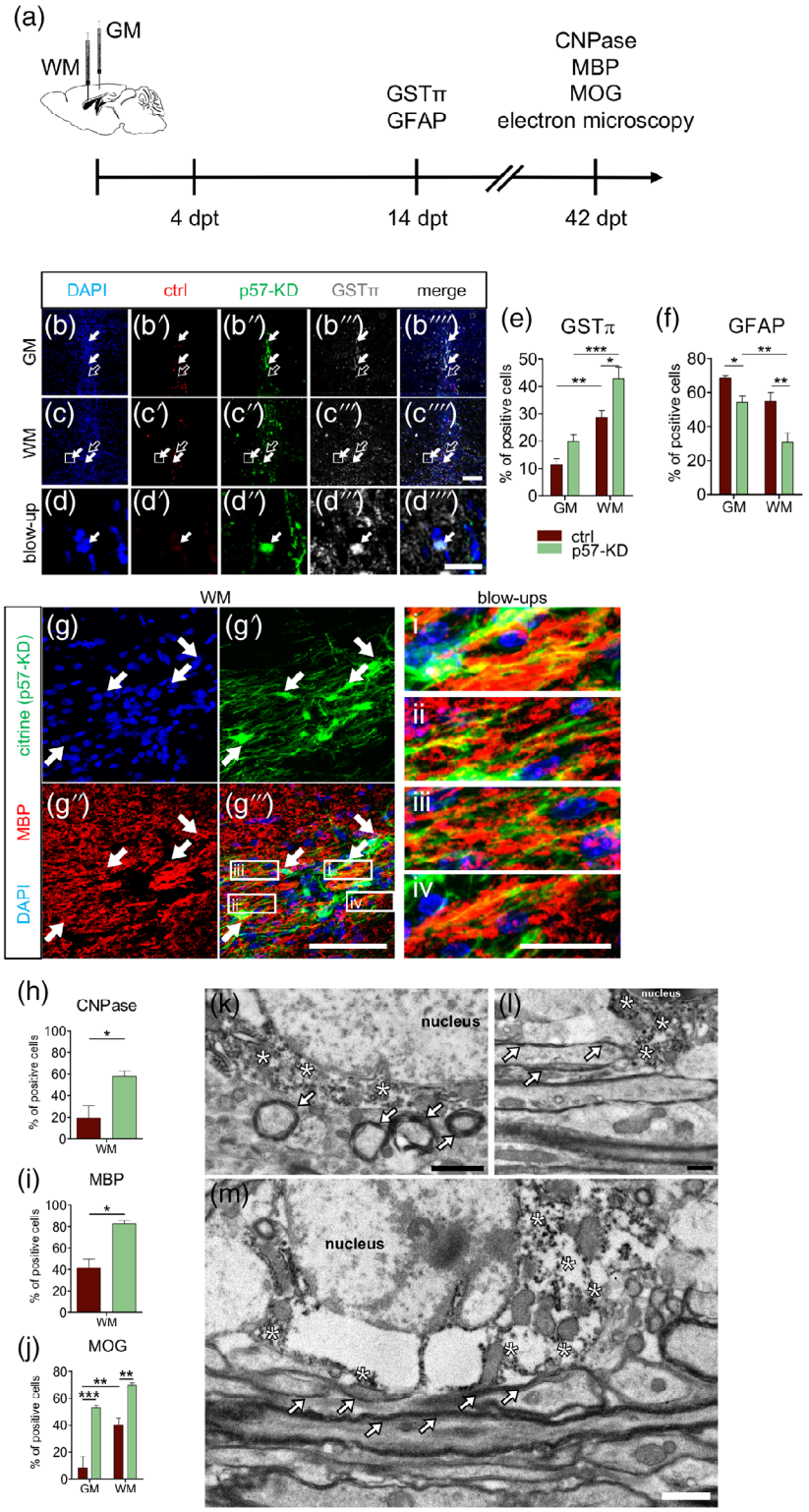

FIGURE 5 Suppression of p57kip2 leads to an increased yield of adult NSC-derived myelinating oligodendrocytes. (a) aNSC transplantation set up into GM or WM, time points and examined marker proteins (ctrl: tdTomato-only-positive nontransfected cells; p57-KD: citrine-positive p57kip2 suppressed cells). (b–e) Immunohistochemical analysis 14 days posttransplantation revealed that the ratio of GSTπ expressing cells was increased in WM and upon p57kip2 suppression. (f) At the same time, less transplanted aNSCs differentiated into GFAP expressing astrocytes. Immunohistochemical assessment of myelin protein expressing cells in the corpus callosum 42 days after transplantation revealed significant increases in CNPase- (h), MBP- (g–g‴), and MOG-positive cells (j) following p57kip2 suppression (green bars). Inserts in (c–c‴) and (g‴) correspond to blow-ups in (d–d‴) and (i–iv), respectively. White rectangles in (g‴) surround MBP-positive processes of transplanted p57-KD aNSC in the corpus callosum. White arrows point toward citrine- and GSTπ- (b-d‴) or MBP- (g–g‴) double-positive cells. (k–m) Electron microscopy images show that p57-KD cells after 42 days posttransplantation exhibit anti-GFP staining-derived electron dense precipitates in the cytoplasm of myelinating extension (asterisks) and are in direct proximity to myelinated axons (arrows) in the corpus callosum. Data are shown as mean values, error bars represent *SEM*. Number of independent experiments: *n* = four animals per graft site for (e,f,j) and *n* = three animals for (h,i). Statistical significance was calculated using Student's two-sided, unpaired *t* test (h,i) and using two-way ANOVA with Bonferroni posttest (e,f,j): **p* < .05; ***p* < .01; ****p* < .001. Scale bar in (c‴,g‴): 100 μm, scale bar in (d‴): 20 μm, scale bar in (iv): 25 μm, scale bar in (k,l): 1 μm, scale bar in (m): 500 nm. ANOVA, analysis of variance; aNSCs, adult neural stem cells; GFAP, glial fibrillary acidic protein; GM, gray matter; GSTπ, glutathione-S-transferase-π; MBP, myelin basic protein; WM, white matter [Color figure can be viewed at wileyonlinelibrary.com]

(an overview of such a lesion and citrine-positive transplanted cells [green] is shown in Supplementary Figure 4) was chosen and SVZ-derived rat aNSCs were used according to our previous study (Jadasz et al., 2012). Here, either empty vector control transfected- (ctrl) or p57kip2-suppressed (p57-KD) aNSCs were transplanted into GM and WM rostral and caudal to the lesion site, immediately after spinal cords were hemisectioned (Figure 6a). In contrast to our observations on mouse brain implanted stem cells, the average number of transplanted and surviving cells in the lesioned spinal cord significantly dropped in response to the p57kip2 knockdown at 7 dpt (Figure 6b). Immunofluorescent staining revealed no difference in the extent of Sox10-positivity in control cells between GM and WM and a significantly increased degree of Sox10-positivity in p57-KD cells transplanted into WM tracts (Figure 6c–h″,i). The number of GSTπ

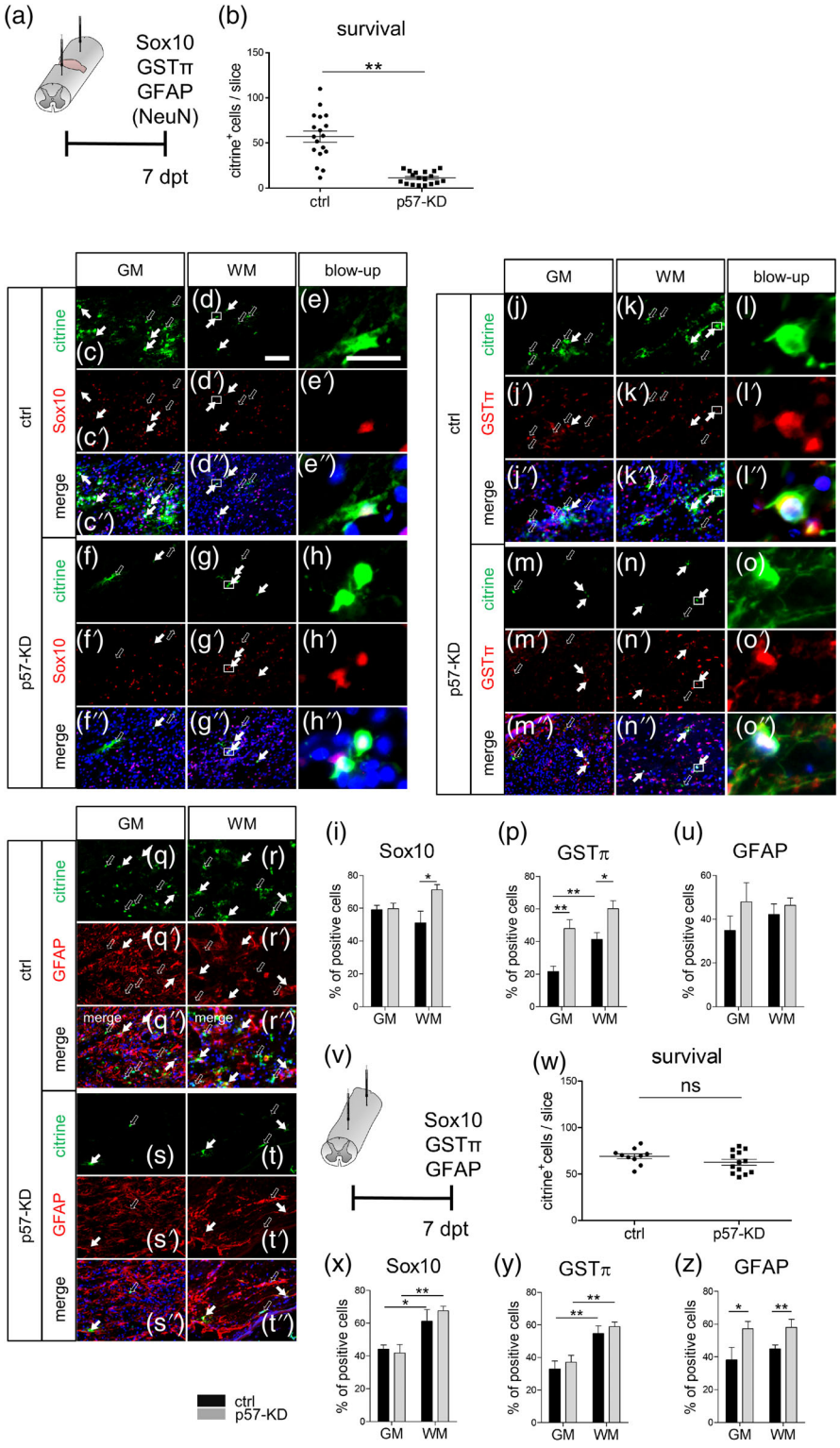

FIGURE 6 High vulnerability of aNSC-derived oligodendroglial cells in the spinal cord injury microenvironment. (a) Hemisected rat spinal cord transplantation set up, time point, and examined marker proteins (ctrl: control transfected cells [black bars]; p57-KD: p57kip2 suppressed cells [gray bars]; both populations marked by means of citrine cotransfection). (b) Cell survival was negatively affected in the p57-KD aNSC population. (c–u) Immunohistochemical analyses for Sox10, GSTπ, and GFAP 7 days posttransplantation. Inserts in (d–d″), (g–g″), (k–k″), and (n–n″) correspond to blow-ups shown in (e–e″), (h–h″), (l–l″), and (o–o″), respectively. White arrows point toward citrine- and Sox10-/GSTπ-/GFAP- double-positive cells, respectively, while open arrows point toward citrine-positive cells only. Scale bar in (d) for all nonmagnified pictures: 100 μm. Scale bar in (e) for all blow-up pictures: 20 μm. (v) Transplantation set up into the noninjured rat spinal cord, time point, and examined marker proteins (ctrl: control transfected cells [black bars]; p57-KD: p57kip2 suppressed cells [gray bars]; both populations marked by means of citrine cotransfection). (w) Cell survival of p57-KD and ctrl-transfected cells was not affected in the lesion-free transplantation paradigm. (x–z) In the intact spinal cord transplantation set up, the p57-KD cell population showed low (z) or no (x,y) pro-glial differentiation compared to the control aNSCs. However, transplantation into WM resulted in a significantly increased number of oligodendroglial cells compared to GM grafts (x,y). Data are shown as mean values, error bars represent *SEM*. Number of independent experiments: n = 6 control- versus 5 p57-KD animals for hemisected animals and 4 control- versus 5 p57-KD animals for transplantation into the noninjured spinal cord. Statistical significance was calculated using Student's two-sided, unpaired t test (b,w) and using two-way ANOVA with Bonferroni posttest (i,p,u,x–z): $*p < .05$; $**p < .01$. aNSCs, adult neural stem cells; GFAP, glial fibrillary acidic protein; GM, gray matter; GSTπ, glutathione-S-transferase-π; WM, white matter [Color figure can be viewed at wileyonlinelibrary.com]

protein-positive transplanted stem cells was increased by the p57kip2 knockdown in both, GM as well as WM (Figure 6j–o″,p) with the highest ratio of GSTπ-positive aNSC-derived cells to be found upon gene knockdown in the WM area. While we showed that in the intact (or mildly traumatically affected) mouse brain the impact of WM as well as of the p57kip2-knockdown leads to a reduced astrocyte generation, staining for GFAP expression in spinal cord implanted stem cells revealed almost no change in the extent of this marker expression (Figure 6q–t″,u). In line with the observation that none of the transplanted aNSCs were found expressing the neuronal marker NeuN (data not shown), it can be concluded that almost exclusively glial derivates arose from grafted stem cells, probably due to the astrogenic environment (Beyer, Samper Agrelo, & Küry, 2019 and references therein). Note that since in the lesion paradigm we decided to

perform our analyses at 7 dpt, so considerably later than in the brain (4 dpt), neuron detection was carried out using NeuN as marker. This goes along with the finding that for control- as well as for p57-KD cells, respective proportions of GFAP- and Sox10-positive cells added up close to 100% in both GM and WM. In contrast to our findings of reduced numbers of citrine-positive/p57kip2 suppressed cells in the vicinity of hemisectioned spinal cords (Figure 6b), survival rates between transplanted control- and p57-KD aNSCs did not differ in the nonlesioned spinal cord (Figure 6w). Here, we found that a total number of 686.9 ± 27.3 p57-KD cells and 662.4 ± 29.9 ctrl cells survived and integrated into the host tissue at 7 dpt. Moreover, upon transplantation into the intact spinal cord no profound pro-oligodendroglial effect in response to suppression of p57kip2 was observed as assessed using markers such as Sox10 and GSTπ (Figure 6x,y). The extent of GFAP-positive cells was comparable in lesioned and nonlesioned tissues (Figure 6u,z) with a differentiation effect upon knockdown of p57kip2 resulting in a slight increase in GFAP-positive astrocytes after transplantation in the lesion-free spinal cord. However, aNSCs transplanted into the WM still showed increased oligodendroglial marker expression as compared to GM transplants (Figure 6x,y).

4 | DISCUSSION

An assessment of glial heterogeneity within the CNS is an important yet unsolved aspect of cell lineage analysis and for myelinating cells, it includes the description of different oligodendroglial cell populations within different brain regions (Vigano et al., 2013), during development (Spitzer et al., 2019) or in demyelinating diseases (Jäkel et al., 2019). Vigano et al., for example, reported an impaired differentiation of GM-derived OPCs compared to WM-derived OPCs upon heterotopic transplantation into GM and WM suggesting intrinsic differences between adult OPC subpopulations to occur (Vigano et al., 2013). Furthermore, they demonstrated that the WM environment can help to overcome intrinsic inhibitory cues acting on GM OPCs providing evidence for a role of differentially expressed extracellular matrix and/or diffusible ligands. Additional impact results from the contribution of aNSCs being heterogeneous between not only different niches but also revealing variations within well-defined niches such as the SVZ (Mizrak et al., 2019). For OPCs and aNSCs, overlapping intrinsic regulators of oligodendroglial differentiation have been described, such as, for example, Sox10, Olig2, and p57kip2 (Copray et al., 2006; Jadasz et al., 2012; Pozniak et al., 2010). Yet, it remains to be shown whether overall differentiation and maturation processes are really identical and to what degree progenitor or stem cell derivatives depend on environmental cues. The latter fact is also important considering the observation that internodes in remyelinated animals differ in terms of length and thickness depending on the origin of the myelinating cells (Xing et al., 2014). In order to achieve a better understanding of how aNSCs can contribute to glial cell heterogeneity either in different brain regions or under hostile conditions and to see whether extrinsic signals can be overcome by intrinsic manipulation of the stem cell fate choice, we transplanted genetically modulated aNSCs in different CNS regions of mice and rats. By using less committed neural stem cells (as compared to committed OPCs), we aimed to reveal the full potential of healthy and lesioned GM- versus WM-derived heterogeneous signals on cell fate acquisition and integration.

Our data clearly demonstrated that mouse and rat neural stem cells equally respond to lowered p57kip2 expression levels in that this manipulation increased the establishment of oligodendroglial features, improved and accelerated the generation of myelinating oligodendroglial cells at the expense of astroglial marker expression. Such directed fate acquisition and differentiation appeared to dominate over tissue specific cues such as in GM areas of the brain, where oligodendroglial fate directing cues seem to be either limited or of inhibitory nature. Moreover, increased oligodendroglial differentiation upon transplantation into WM tracts was further enhanced by the intrinsic p57kip2 modulation, which additionally granted a survival benefit resulting in a much higher yield of myelinating aNSC-derived oligodendrocytes. Of note, neuronal differentiation was not observed in cultured cells and following transplantation, no differences in the extent of neurogenesis were observed. Whereas in stem cell culture this is likely to result from the astroglial promoting medium hence conferring a restriction to glial decisions it can be concluded that in vivo p57kip2 does not influence neurogenesis in this context.

Experimental transplantation of NSCs into CNS tissue aiming either at directed cell replacement or the local generation of trophic signals has so far almost exclusively been conducted under pathophysiological conditions (Assinck, Duncan, Hilton, Plemel, & Tetzlaff, 2017; Beyer et al., 2019). Few studies only engaged into regional differences (Fricker et al., 1999; Gage et al., 1995; Herrera, Garcia-Verdugo, & Alvarez-Buylla, 1999; Seidenfaden, Desoeuvre, Bosio, Virard, & Cremer, 2006) and none of them considered a potential impact of GM versus WM on implanted stem cells. Overall, the currently published injury- and pathology-free CNS transplantation studies imply that transplanted NSCs do sense their ectopic environment and to some degree adapt environment-specific migratory features and fate acquisition (summarized in Beyer et al. (2019)). However, direct assessment of GM versus WM differences on NCS fate and a detailed overview of oligodendroglial differentiation over time has so far been missing.

The here described differences observed between GM and WM of healthy and lesioned CNS point to dominant roles of an intrinsic fate modulation (here by suppression of p57kip2) and WM signals regarding oligodendroglial fate acquisition and successful execution of differentiation programs in the healthy CNS and of injury environmental cues related to cell survival. Based on these observations, particularly taking into account lowered long-term survival rates among GM grafts, it can be concluded that therapeutic cell replacement strategies either should be limited to diseases with a clear WM impact or must consider additional survival promoting manipulations. The absent pro-oligodendroglial effect in response to p57kip2 knockdown in the healthy spinal cord differed from our observations in the healthy brain. Several reasons might account for these differences such as, for

example, myelination dynamics and myelin as well as oligodendrocyte turnover not being identical over all CNS regions (Foran & Peterson, 1992; Snaidero & Simons, 2014; Williamson & Lyons, 2018). Further, we have to acknowledge that the composition of both tissues and their signaling cues affecting NSC fate and differentiation might differ. Finally, we cannot rule out species differences between our two rodent transplantation models. This can be interpreted in that p57kip2 suppression driven pro-oligodendroglial differentiation and cell integration can only be seen in tissues with a certain need for (re) myelination. Another question to be solved in the future relates to the heterogeneity among SVZ aNSCs (Azim et al., 2018) which might have an impact on how receptive these cells respond to an intrinsic p57kip2 modulation or extrinsic cues upon transplantation. Whether this includes for example the expression of a specific subset of gap junction proteins such as connexins would be of interest to address. Dynamic connexin expression following transplantation into striatal slice cultures and the generation of connexin-dependent networks were reported to affect adult neural precursor survival (Jaderstad, Jaderstad, & Herlenius, 2011; Ravella, Ringstedt, Brion, Pandolfo, & Herlenius, 2015). To what degree observed dependencies also apply to endogenous stem cells naturally giving rise to new oligodendrocytic cells, hence in a noninvasive experimental paradigm, thus most likely limited to myelin repair in demyelinating conditions, needs to be addressed in future experiments.

Taking other transplantation studies into account, it appears that the number of surviving NSCs seems to be overall rather low (as exemplified in Herrera et al. (1999), Raedt et al. (2009), and Seidenfaden et al. (2006)); summarized in Beyer et al. (2019)). It is therefore of considerable interest to see that suppression of the intrinsic regulator p57kip2 imparts a survival benefit. This might indeed be promising in light of improving potential myelinating cell replacement strategies. However, we also found that the number of p57kip2 suppressed cells was severely reduced upon grafting into lesioned CNS tissue suggesting that a promoted oligodendroglial fate acquisition on the one hand facilitates successful tissue integration but on the other hand might come with an increased sensitivity toward hostile cues as described before (Casha, Yu, & Fehlings, 2001; Crowe, Bresnahan, Shuman, Masters, & Beattie, 1997; Pfeifer et al., 2006; Rowland, Hawryluk, Kwon, & Fehlings, 2008; Vroemen, Aigner, Winkler, & Weidner, 2003). An influence of spinal cord infiltrating peripheral immune cells (Anderson, 2002; Margul et al., 2016) can also not be excluded yet. Such an impact could only be addressed by future transplantation experiments into subacute spinal cord injuries at later time points featuring reduced inflammation and beyond secondary cell death. Changes toward less hostile lesion conditions have in fact already been described for transplanted NSCs in temporal lobe epilepsy models (Raedt et al., 2009). However, it remains to be seen to what degree such a delayed aNSC application makes sense as grafting into lesion regions primarily aims at protection of demyelinated/endangered axons. In this regard, cotransplantation of NSCs with other cells that can exert an overall benefit to the whole lesion environment such as mediated by unrestricted somatic stem cells (Schira et al., 2012) or mesenchymal stem cells (Jadasz et al., 2012; Jadasz et al., 2018) might therefore constitute a promising alternative approach. Of note, cotransplantations of NSCs with other cells revealed indeed to be beneficial in terms of cell survival and functional improvements in ischemic stroke animal models (Cai et al., 2015; Luo et al., 2017). Moreover, coapplication of blockers of spinal cord injury-evoked oligodendroglia hostile cues such as chondroitin sulfate proteoglycans (Dyck, Kataria, Akbari-Kelachayeh, Silver, & Karimi-Abdolrezaee, 2019) might further increase the yield in p57-KD aNSC-derived oligodendrocytes.

In conclusion, our work uncovered regional heterogeneity between rodent CNS GM and WM affecting survival and fate of transplanted aNSCs. Here, WM tissue substantially promoted both, survival as well as differentiation into myelinating oligodendrocytes. In addition, we showed that suppression of the p57kip2 gene further increased WM effects and in part antagonized lower oligodendroglial yield in GM grafts. Gene knockdown-promoted oligodendrogenesis, however, suffers from a negative impact on cell survival mediated by the injured CNS hostile microenvironment, which must therefore be addressed prior to future cell replacement therapies.

ACKNOWLEDGMENTS

The thank Birgit Blomenkamp, Marion Hendricks, Julia Jadasz, Zippora Kohne, Brigida Ziegler (all Düsseldorf), and Heinrich Blazyca (Würzburg) for their technical assistance and Prof. Dr. Olga Sergeeva for providing tdTomato reporter mouse line. This study was supported by the Deutsche Forschungsgemeinschaft (DFG; grants KU1934/2–1 and KU1934/5–1). Research on myelin repair and neuroregeneration has also been supported by the Christiane and Claudia Hempel Foundation for clinical stem cell research, DMSG Ortsvereinigung Düsseldorf und Umgebung e.V., iBrain, Stifterverband/Novartisstiftung, and Peek & Cloppenburg Düsseldorf Stiftung. The MS Center at the Department of Neurology is supported in part by the Walter and Ilse Rose Foundation.

CONFLICT OF INTEREST

The authors declare that there is no conflict of interests regarding the publication of this article.

ETHICS STATEMENT

Rodent primary stem cell preparation was approved by the ZETT (Zentrale Einrichtung für Tierforschung und wissenschaftliche Tierschutzaufgaben; O90/15, O118/11). Cell transplantation experiments presented were approved by the authorities LANUV (Landesamt für Natur, Umwelt und Verbraucherschutz Nordrhein-Westfalen; Az.: 84-02.04.2015.A239; Az.: 84-02.04.2015.A525).

DATA AVAILABILITY STATEMENT

The data that support the findings of this study are available from the corresponding author upon reasonable request.

ORCID

Felix Beyer https://orcid.org/0000-0002-3329-0249
Janusz Jadasz https://orcid.org/0000-0002-5505-4570
Janos Groh https://orcid.org/0000-0002-7628-0163
Julio Vera https://orcid.org/0000-0002-3076-5122
Patrick Küry https://orcid.org/0000-0002-2654-1126

REFERENCES

Akkermann, R., Beyer, F., & Küry, P. (2017). Heterogeneous populations of neural stem cells contribute to myelin repair. *Neural Regeneration Research*, *12*(4), 509–517. https://doi.org/10.4103/1673-5374.204999

Anderson, A. J. (2002). Mechanisms and pathways of inflammatory responses in CNS trauma: Spinal cord injury. *The Journal of Spinal Cord Medicine*, *25*(2), 70–79 discussion 80.

Assinck, P., Duncan, G. J., Hilton, B. J., Plemel, J. R., & Tetzlaff, W. (2017). Cell transplantation therapy for spinal cord injury. *Nature Neuroscience*, *20*(5), 637–647. https://doi.org/10.1038/nn.4541

Azim, K., Akkermann, R., Cantone, M., Vera, J., Jadasz, J. J., & Küry, P. (2018). Transcriptional profiling of ligand expression in cell specific populations of the adult mouse forebrain that regulates neurogenesis. *Frontiers in Neuroscience*, *12*, 220. https://doi.org/10.3389/fnins.2018.00220

Beyer, F., Samper Agrelo, I., & Küry, P. (2019). Do neural stem cells have a choice? Heterogenic outcome of cell fate acquisition in different injury models. *International Journal of Molecular Sciences*, *20*(2), 455. https://doi.org/10.3390/ijms20020455

Bond, A. M., Ming, G. L., & Song, H. (2015). Adult mammalian neural stem cells and neurogenesis: Five decades later. *Cell Stem Cell*, *17*(4), 385–395. https://doi.org/10.1016/j.stem.2015.09.003

Brousse, B., Magalon, K., Durbec, P., & Cayre, M. (2015). Region and dynamic specificities of adult neural stem cells and oligodendrocyte precursors in myelin regeneration in the mouse brain. *Biology Open*, *4*(8), 980–992. https://doi.org/10.1242/bio.012773

Cai, Q., Chen, Z., Song, P., Wu, L., Wang, L., Deng, G., … Chen, Q. (2015). Co-transplantation of hippocampal neural stem cells and astrocytes and microvascular endothelial cells improve the memory in ischemic stroke rat. *International Journal of Clinical and Experimental Medicine*, *8*(8), 13109–13117.

Casha, S., Yu, W. R., & Fehlings, M. G. (2001). Oligodendroglial apoptosis occurs along degenerating axons and is associated with FAS and p75 expression following spinal cord injury in the rat. *Neuroscience*, *103*(1), 203–218.

Copray, S., Balasubramaniyan, V., Levenga, J., de Bruijn, J., Liem, R., & Boddeke, E. (2006). Olig2 overexpression induces the in vitro differentiation of neural stem cells into mature oligodendrocytes. *Stem Cells*, *24*(4), 1001–1010. https://doi.org/10.1634/stemcells.2005-0239

Crowe, M. J., Bresnahan, J. C., Shuman, S. L., Masters, J. N., & Beattie, M. S. (1997). Apoptosis and delayed degeneration after spinal cord injury in rats and monkeys. *Nature Medicine*, *3*(1), 73–76. https://doi.org/10.1038/nm0197-73

Duncan, I. D., Radcliff, A. B., Heidari, M., Kidd, G., August, B. K., & Wierenga, L. A. (2018). The adult oligodendrocyte can participate in remyelination. *Proceedings of the National Academy of Sciences of the United States of America*, *115*(50), E11807–E11816. https://doi.org/10.1073/pnas.1808064115

Dyck, S., Kataria, H., Akbari-Kelachayeh, K., Silver, J., & Karimi-Abdolrezaee, S. (2019). LAR and PTP sigma receptors are negative regulators of oligodendrogenesis and oligodendrocyte integrity in spinal cord injury. *Glia*, *67*(1), 125–145. https://doi.org/10.1002/glia.23533

Falcao, A. M., van Bruggen, D., Marques, S., Meijer, M., Jakel, S., Agirre, E., … Castelo-Branco, G. (2018). Disease-specific oligodendrocyte lineage cells arise in multiple sclerosis. *Nature Medicine*, *24*(12), 1837–1844. https://doi.org/10.1038/s41591-018-0236-y

Foran, D. R., & Peterson, A. C. (1992). Myelin acquisition in the central nervous system of the mouse revealed by an MBP-Lac Z transgene. *The Journal of Neuroscience*, *12*(12), 4890–4897.

Fricker, R. A., Carpenter, M. K., Winkler, C., Greco, C., Gates, M. A., & Bjorklund, A. (1999). Site-specific migration and neuronal differentiation of human neural progenitor cells after transplantation in the adult rat brain. *The Journal of Neuroscience*, *19*(14), 5990–6005.

Gage, F. H., Coates, P. W., Palmer, T. D., Kuhn, H. G., Fisher, L. J., Suhonen, J. O., … Ray, J. (1995). Survival and differentiation of adult neuronal progenitor cells transplanted to the adult brain. *Proceedings of the National Academy of Sciences of the United States of America*, *92*(25), 11879–11883.

Göttle, P., Manousi, A., Kremer, D., Reiche, L., Hartung, H. P., & Küry, P. (2018). Teriflunomide promotes oligodendroglial differentiation and myelination. *Journal of Neuroinflammation*, *15*(1), 76. https://doi.org/10.1186/s12974-018-1110-z

Göttle, P., Sabo, J. K., Heinen, A., Venables, G., Torres, K., Tzekova, N., … Küry, P. (2015). Oligodendroglial maturation is dependent on intracellular protein shuttling. *The Journal of Neuroscience*, *35*(3), 906–919. https://doi.org/10.1523/jneurosci.1423-14.2015

Heinen, A., Kremer, D., Göttle, P., Kruse, F., Hasse, B., Lehmann, H., … Küry, P. (2008). The cyclin-dependent kinase inhibitor p57kip2 is a negative regulator of Schwann cell differentiation and in vitro myelination. *Proceedings of the National Academy of Sciences of the United States of America*, *105*(25), 8748–8753. https://doi.org/10.1073/pnas.0802659105

Herrera, D. G., Garcia-Verdugo, J. M., & Alvarez-Buylla, A. (1999). Adult-derived neural precursors transplanted into multiple regions in the adult brain. *Annals of Neurology*, *46*(6), 867–877.

Imayoshi, I., Ohtsuka, T., Metzger, D., Chambon, P., & Kageyama, R. (2006). Temporal regulation of Cre recombinase activity in neural stem cells. *Genesis*, *44*(5), 233–238. https://doi.org/10.1002/dvg.20212

Jadasz, J. J., Rivera, F. J., Taubert, A., Kandasamy, M., Sandner, B., Weidner, N., … Küry, P. (2012). p57kip2 regulates glial fate decision in adult neural stem cells. *Development*, *139*(18), 3306–3315. https://doi.org/10.1242/dev.074518

Jadasz, J. J., Tepe, L., Beyer, F., Samper Agrelo, I., Akkermann, R., Spitzhorn, L. S., … Küry, P. (2018). Human mesenchymal factors induce rat hippocampal- and human neural stem cell dependent oligodendrogenesis. *Glia*, *66*(1), 145–160. https://doi.org/10.1002/glia.23233

Jaderstad, J., Jaderstad, L. M., & Herlenius, E. (2011). Dynamic changes in connexin expression following engraftment of neural stem cells to striatal tissue. *Experimental Cell Research*, *317*(1), 70–81. https://doi.org/10.1016/j.yexcr.2010.07.011

Jäkel, S., Agirre, E., Mendanha Falcão, A., van Bruggen, D., Lee, K. W., Knuesel, I., … Castelo-Branco, G. (2019). Altered human oligodendrocyte heterogeneity in multiple sclerosis. *Nature*, *566*(7745), 543–547. https://doi.org/10.1038/s41586-019-0903-2

Koutsoudaki, P. N., Papastefanaki, F., Stamatakis, A., Kouroupi, G., Xingi, E., Stylianopoulou, F., & Matsas, R. (2016). Neural stem/progenitor cells differentiate into oligodendrocytes, reduce inflammation, and ameliorate learning deficits after transplantation in a mouse model of traumatic brain injury. *Glia*, *64*(5), 763–779. https://doi.org/10.1002/glia.22959

Kremer, D., Heinen, A., Jadasz, J., Göttle, P., Zimmermann, K., Zickler, P., … Küry, P. (2009). p57kip2 is dynamically regulated in experimental autoimmune encephalomyelitis and interferes with oligodendroglial maturation. *Proceedings of the National Academy of Sciences of the United States of America*, *106*(22), 9087–9092. https://doi.org/10.1073/pnas.0900204106

Lentferink, D. H., Jongsma, J. M., Werkman, I., & Baron, W. (2018). Grey matter OPCs are less mature and less sensitive to IFN gamma than white matter OPCs: Consequences for remyelination. *Scientific Reports*, *8*(1), 2113. https://doi.org/10.1038/s41598-018-19934-6

Lim, D. A., & Alvarez-Buylla, A. (2016). The adult ventricular-subventricular zone (V-SVZ) and olfactory bulb (OB) neurogenesis. *Cold Spring Harbor Perspectives in Biology*, *8*(5), a018820. https://doi.org/10.1101/cshperspect.a018820

Luo, L., Guo, K., Fan, W., Lu, Y., Chen, L., Wang, Y., … Lu, L. (2017). Niche astrocytes promote the survival, proliferation and neuronal differentiation of co-transplanted neural stem cells following ischemic stroke in rats. *Experimental and Therapeutic Medicine*, *13*(2), 645–650. https://doi.org/10.3892/etm.2016.4016

Margul, D. J., Park, J., Boehler, R. M., Smith, D. R., Johnson, M. A., McCreedy, D. A., … Seidlits, S. K. (2016). Reducing neuroinflammation by delivery of IL-10 encoding lentivirus from multiple-channel bridges. *Bioengineering & Translational Medicine*, *1*(2), 136–148. https://doi.org/10.1002/btm2.10018

Marques, S., Zeisel, A., Codeluppi, S., van Bruggen, D., Mendanha Falcao, A., Xiao, L., … Castelo-Branco, G. (2016). Oligodendrocyte heterogeneity in the mouse juvenile and adult central nervous system. *Science*, *352*(6291), 1326–1329. https://doi.org/10.1126/science.aaf6463

Menn, B., Garcia-Verdugo, J. M., Yaschine, C., Gonzalez-Perez, O., Rowitch, D., & Alvarez-Buylla, A. (2006). Origin of oligodendrocytes in the subventricular zone of the adult brain. *The Journal of Neuroscience*, *26*(30), 7907–7918. https://doi.org/10.1523/JNEUROSCI.1299-06.2006

Miltiadous, P., Kouroupi, G., Stamatakis, A., Koutsoudaki, P. N., Matsas, R., & Stylianopoulou, F. (2013). Subventricular zone-derived neural stem cell grafts protect against hippocampal degeneration and restore cognitive function in the mouse following intrahippocampal kainic acid administration. *Stem Cells Translational Medicine*, *2*(3), 185–198. https://doi.org/10.5966/sctm.2012-0074

Mizrak, D., Levitin, H. M., Delgado, A. C., Crotet, V., Yuan, J., Chaker, Z., … Doetsch, F. (2019). Single-cell analysis of regional differences in adult V-SVZ neural stem cell lineages. *Cell Reports*, *26*(2), 394–406 e395. https://doi.org/10.1016/j.celrep.2018.12.044

Nait-Oumesmar, B., Decker, L., Lachapelle, F., Avellana-Adalid, V., Bachelin, C., & Baron-Van Evercooren, A. (1999). Progenitor cells of the adult mouse subventricular zone proliferate, migrate and differentiate into oligodendrocytes after demyelination. *The European Journal of Neuroscience*, *11*(12), 4357–4366.

Nait-Oumesmar, B., Picard-Riera, N., Kerninon, C., Decker, L., Seilhean, D., Hoglinger, G. U., … Baron-Van Evercooren, A. (2007). Activation of the subventricular zone in multiple sclerosis: Evidence for early glial progenitors. *Proceedings of the National Academy of Sciences of the United States of America*, *104*(11), 4694–4699. https://doi.org/10.1073/pnas.0606835104

Pfeifer, K., Vroemen, M., Caioni, M., Aigner, L., Bogdahn, U., & Weidner, N. (2006). Autologous adult rodent neural progenitor cell transplantation represents a feasible strategy to promote structural repair in the chronically injured spinal cord. *Regenerative Medicine*, *1*(2), 255–266. https://doi.org/10.2217/17460751.1.2.255

Picard-Riera, N., Decker, L., Delarasse, C., Goude, K., Nait-Oumesmar, B., Liblau, R., … Baron-Van Evercooren, A. (2002). Experimental autoimmune encephalomyelitis mobilizes neural progenitors from the subventricular zone to undergo oligodendrogenesis in adult mice. *Proceedings of the National Academy of Sciences of the United States of America*, *99*(20), 13211–13216. https://doi.org/10.1073/pnas.192314199

Pozniak, C. D., Langseth, A. J., Dijkgraaf, G. J., Choe, Y., Werb, Z., & Pleasure, S. J. (2010). Sox10 directs neural stem cells toward the oligodendrocyte lineage by decreasing suppressor of fused expression. *Proceedings of the National Academy of Sciences of the United States of America*, *107*(50), 21795–21800. https://doi.org/10.1073/pnas.1016485107

Raedt, R., Van Dycke, A., Waeytens, A., Wyckhuys, T., Vonck, K., Wadman, W., & Boon, P. (2009). Unconditioned adult-derived neurosphere cells mainly differentiate towards astrocytes upon transplantation in sclerotic rat hippocampus. *Epilepsy Research*, *87*(2–3), 148–159. https://doi.org/10.1016/j.eplepsyres.2009.08.009

Ravella, A., Ringstedt, T., Brion, J.-P., Pandolfo, M., & Herlenius, E. (2015). Adult neural precursor cells form connexin-dependent networks that improve their survival. *Neuroreport*, *26*(15), 928–936. https://doi.org/10.1097/WNR.0000000000000451

Rowland, J. W., Hawryluk, G. W., Kwon, B., & Fehlings, M. G. (2008). Current status of acute spinal cord injury pathophysiology and emerging therapies: Promise on the horizon. *Neurosurgical Focus*, *25*(5), E2. https://doi.org/10.3171/FOC.2008.25.11.E2

Schira, J., Gasis, M., Estrada, V., Hendricks, M., Schmitz, C., Trapp, T., … Muller, H. W. (2012). Significant clinical, neuropathological and behavioural recovery from acute spinal cord trauma by transplantation of a well-defined somatic stem cell from human umbilical cord blood. *Brain*, *135*(Pt. 2), 431–446. https://doi.org/10.1093/brain/awr222

Seidenfaden, R., Desoeuvre, A., Bosio, A., Virard, I., & Cremer, H. (2006). Glial conversion of SVZ-derived committed neuronal precursors after ectopic grafting into the adult brain. *Molecular and Cellular Neurosciences*, *32*(1–2), 187–198. https://doi.org/10.1016/j.mcn.2006.04.003

Snaidero, N., & Simons, M. (2014). Myelination at a glance. *Journal of Cell Science*, *127*(14), 2999–3004. https://doi.org/10.1242/jcs.151043

Spitzer, S. O., Sitnikov, S., Kamen, Y., Evans, K. A., Kronenberg-Versteeg, D., Dietmann, S., … Karadottir, R. T. (2019). Oligodendrocyte progenitor cells become regionally diverse and heterogeneous with age. *Neuron*, *101*(3), 459–471 e455. https://doi.org/10.1016/j.neuron.2018.12.020

Vigano, F., Möbius, W., Götz, M., & Dimou, L. (2013). Transplantation reveals regional differences in oligodendrocyte differentiation in the adult brain. *Nature Neuroscience*, *16*(10), 1370–1372. https://doi.org/10.1038/nn.3503

Vroemen, M., Aigner, L., Winkler, J., & Weidner, N. (2003). Adult neural progenitor cell grafts survive after acute spinal cord injury and integrate along axonal pathways. *The European Journal of Neuroscience*, *18*(4), 743–751.

Williamson, J. M., & Lyons, D. A. (2018). Myelin dynamics throughout life: An ever-changing landscape? *Frontiers in Cellular Neuroscience*, *12*, 424. https://doi.org/10.3389/fncel.2018.00424

Xing, Y. L., Roth, P. T., Stratton, J. A., Chuang, B. H., Danne, J., Ellis, S. L., … Merson, T. D. (2014). Adult neural precursor cells from the subventricular zone contribute significantly to oligodendrocyte regeneration and remyelination. *The Journal of Neuroscience*, *34*(42), 14128–14146. https://doi.org/10.1523/JNEUROSCI.3491-13.2014

Yeung, M. S. Y., Djelloul, M., Steiner, E., Bernard, S., Salehpour, M., Possnert, G., … Frisen, J. (2019). Dynamics of oligodendrocyte generation in multiple sclerosis. *Nature*, *566*(7745), 538–542. https://doi.org/10.1038/s41586-018-0842-3

SUPPORTING INFORMATION

Additional supporting information may be found online in the Supporting Information section at the end of this article.

How to cite this article: Beyer F, Jadasz J, Samper Agrelo I, et al. Heterogeneous fate choice of genetically modulated adult neural stem cells in gray and white matter of the central nervous system. *Glia*. 2020;68:393–406. https://doi.org/10.1002/glia.23724